Eur. Phys. J. B **49**, 425–431 (2006)
DOI: 10.1140/epjb/e2006-00081-5

THE EUROPEAN PHYSICAL JOURNAL B

Electronic structure and properties of strontium ferrite $Sr_3Fe_2O_6$

V.M. Zainullina[1,a], M.A. Korotin[2], and V.L. Kozhevnikov[1]

[1] Institute of Solid State Chemistry, 620219 Ekaterinburg GSP-145, Russia
[2] Institute of Metal Physics, 620041 Ekaterinburg GSP-170, Russia

Received 24 May 2005 / Received in final form 30 January 2006
Published online 31 March 2006 –

Abstract. The electronic structure of strontium ferrite $Sr_3Fe_2O_6$ was calculated using the tight-binding linear muffin-tin orbital method (TB LMTO) in the local spin density approximation of density functional theory with Coulomb correlations correction (LSDA+U). The semiconducting character of the spectrum with charge transfer energy gap of 1.82 eV was obtained in reasonably good agreement with experimental data. The iron ions are found to be in the high spin state. The calculated value of the local spin magnetic moment of Fe^{3+} ion is 3.94 μ_B which is not typical for trivalent iron ion in the high spin state. It is shown that the strong hybridization between Fe3d and O2p orbitals favors the d^6L configuration of Fe^{3+} ion, where L is a hole in the oxygen p shell. The mechanism of oxygen transport in ferrite is discussed basing on the total energy calculations of the different spatial configurations of oxygen vacancies.

PACS. 71.20.-b Electron density of states and band structure of crystalline solids – 71.27.+a Strongly correlated electron systems; heavy fermions – 72.10.-d Theory of electronic transport; scattering mechanisms – 75.25.+z Spin arrangements in magnetically ordered materials (including neutron and spin-polarized electron studies, synchrotron-source X-ray scattering, etc.)

1 Introduction

The strontium ferrites $Sr_3Fe_2O_{6+\delta}$ with Ruddlesden-Popper type structure are promising materials for a number of applications [1,2]. The oxygen deficiency δ significantly affects their transport [3–6] and magnetic [6–10] properties. It is known [3,4,6] that $Sr_3Fe_2O_7$ compound is a semiconductor with thermally activated carriers at $T < 340$ K. The oxygen-deficient $Sr_3Fe_2O_{6+\delta}$ and titania-doped derivatives $Sr_3Fe_{2-x}Ti_xO_{6+\delta}$ are mixed ion-electron conductors. They have an energy gap of 2.3 eV, while the activation energy for mobility of both holes and electrons is small [5]. It is known that $Sr_3Fe_2O_7$, $Sr_3Fe_2O_{6.5}$ and $Sr_3Fe_2O_6$ are antiferromagnets with Nèel temperature T_N = 120 K, 150 K and 550 K, respectively [7–9]. The values of effective magnetic moments derived from the Curie-Weiss susceptibility are equal to 4.3 μ_B and 5.3 μ_B for $Sr_3Fe_2O_7$ [6,10] and to 4.39 μ_B for $Sr_3Fe_2O_{6.5}$ [8]. Also the details of long-range magnetic order in these compounds are not yet understood completely. While $Sr_3Fe_2O_{6+\delta}$ compounds with $\delta = 0$ and 0.5 have the spin directions parallel to c axis and magnetic unit cell of $\sqrt{2}a \times \sqrt{2}a \times c$ dimensions [8], for $Sr_3Fe_2O_7$ ferrite the spin direction is *not* parallel to c axis (helical spin structure) and though the size of the real magnetic unit cell is not found exactly. It is suggested in work [6,8] that it is larger than $2a \times 2a \times 4c$.

The electronic structure of $Sr_3Fe_2O_{6+\delta}$ is also studied insufficiently. The analysis of X-ray photoelectron spectra with the using of standard cluster model calculations [11] shows that $Sr_3Fe_2O_7$ compound is in negative charge-transfer regime of band gap formation. This band gap is of p-p type. The ground state is dominated by d^5L configuration (L denotes a p hole in the oxygen band) of Fe^{4+} ions. Any information about electronic structure of oxygen-deficient ($\delta = 0$, 0.5) strontium ferrites, as to our knowledge, is absent. The purpose of this work was to study the electronic structure features in the end member $Sr_3Fe_2O_6$ of this series in order to gain understanding of the physical and chemical properties of the ferrite. For this goal we used self-consistent band structure calculations within the LSDA+U approach.

2 Crystal structure and calculation details

$Sr_3Fe_2O_{6+\delta}$ is known to crystallize with a Ruddlesden-Popper type structure, which is characterized by a two dimensional network of FeO_6 octahedra. The $Sr_3Fe_2O_7$, $Sr_3Fe_2O_{6.5}$, and $Sr_3Fe_2O_6$ compounds are isostructural with oxygen systematically removed from a site linking

[a] e-mail: veronika@ihim.uran.ru

Table 1. Refined atomic parameters for $Sr_3Fe_2O_6$ at room temperature. In the last column, n is site occupancy [12].

Atom	Site	x/a	y/b	z/c	n
Sr(1)	2b	0	0	1/2	1.0
Sr(2)	4e	0	0	0.3193	1.0
Fe	4e	0	0	0.1022	1.0
O(1)	8g	0	1/2	0.0843	1.0
O(2)	4e	0	0	0.1963	1.0
O(3)	2a	0	0	0	0.0

together the FeO_6 octahedra in double layers. The crystal structure of $Sr_3Fe_2O_6$ is tetragonal ($I4/mmm$ space group, No. 139) with $a = 3.8940$ Å, $c = 20.0396$ Å [12]). The atomic positions used in calculations are given in Table 1. The O(3) type oxygen linking octahedra in c direction is absent in $Sr_3Fe_2O_6$. Within each layer every Fe^{3+} atom is connected to four O(1) atoms and one O(2) type oxygen, Figure 1. The iron ion in $Sr_3Fe_2O_6$ has a square pyramidal coordination. The equatorial bond lengths, Fe-O(1), are 1.979 Å and the axial bonds, Fe-O(2), are equal to 1.885 Å.

The electronic structure calculations were carried out with the using of the LSDA+U (local spin density approximation of density functional theory with Coulomb correlations correction) approach [13] within the tight-binding linear muffin-tin orbital method in the atomic sphere approximation (TB LMTO ASA) [14]. The $Sr_6Fe_4O_{12}V_2E_{36}$ supercell was used in calculations, where V denotes an empty sphere (vacancy) in the position of oxygen site O(3) and E is an additional empty sphere. The E spheres were placed into the vacant positions of the lattice because the TB LMTO ASA method was developed for close-packed crystal structures. The basis set of atomic orbitals included 2s, 2p, 3d orbitals of O, 4s, 4p, 3d states of Fe, 5s, 5p, 4d, 4f states of Sr, and 1s, 2p orbitals of V and E. The radius ratios r_{Fe}/r_O and r_{Sr}/r_O were 1.0 and 1.52, respectively with $r_O = 2.1$ a.u. The parameters of Coulomb U and exchange J interactions for localized Fe 3d electrons were chosen after work [15] to be $U = 5$ eV and $J = 1$ eV.

The potentials for the various localized d orbitals of Fe are different in the LSDA+U approach. Therefore, it is not obvious a priori what will be the final symmetry of the solution. Keeping the symmetry during the LSDA+U calculation as high as for the crystal structure, one can fail to detect some (e.g. orbital ordered) solutions. Moreover, in comparison with conventional LSDA approach in which the final magnetic solution, if exists, is unique owing to the same average potential of localized d orbitals, the number of stable magnetic solutions within the LSDA+U approach is not obvious a priori also. Thus, based on the using of appropriate symmetry it is necessary to study the stability of solutions with Fe ions in all possible different spin states including the coexistence of these different spin states in one configuration.

The spin-polarized calculations of strontium ferrite were performed for A, C, and G-type antiferromagnetic

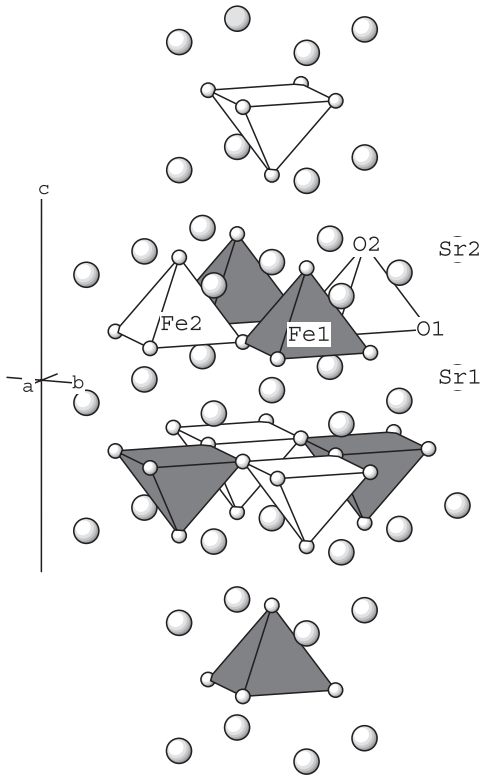

Fig. 1. The crystal structure fragment for $Sr_3Fe_2O_6$. Iron cations Fe1 and Fe2 have oppositely directed spins in the G type AFM structure.

(AFM) orderings of Fe spins in conventional LSDA approach. The type of antiferromagnetic odering is associated with the difference of the spin arrangements between Fe atoms of inter and intra layers. A-type AFM ordering of Fe spins corresponds to ferromagnetic ordering in layers and antiferromagnetic ordering between them. C-type AFM consists of the antiferromagnetic layers with ferromagnetic ordering between the layers. G-AFM ordering characterizes antiferromagnetic interactions between Fe spin of inter and intra layers. The studies of $Sr_3Fe_2O_6$ (G-AFM) compound were carried out in the LSDA+U approximation because this type of AFM order is most energetically favorable in the LSDA and, moreover, just this type corresponds to experimentally determined magnetic unit cell of $\sqrt{2}a \times \sqrt{2}a \times c$ dimensions [8]. In addition, the total energies of $Sr_3Fe_2O_6$ (G-AFM) compounds with different spatial configurations of point defects, such as anti-Frenkel pairs (AFP) and oxygen vacancies, were calculated for understanding the mechanism underlying oxygen transport in the ferrite. The AFP formation energy was defined as the total energy difference between two crystal configurations. One configuration corresponded to the ideal structure of $Sr_3Fe_2O_6$ with two $V_{O(3)}$ vacancies, another did to the defect structure with $V_{O(1)}$ or $V_{O(2)}$ and $V_{O(3)}$ vacancies. All calculations were performed for the lattice without relaxation. The relaxation energy (usually about tens of electron-volts) is smaller then the AFP energy, so probably the lattice relaxation

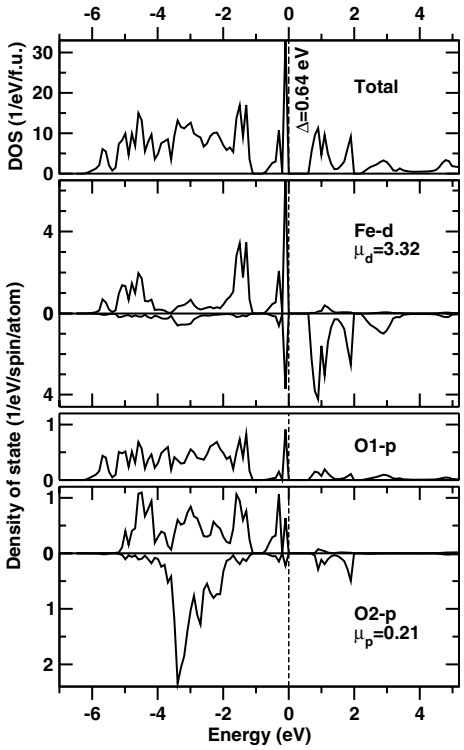

Fig. 2. The total and partial densities of states obtained in LSDA calculations.

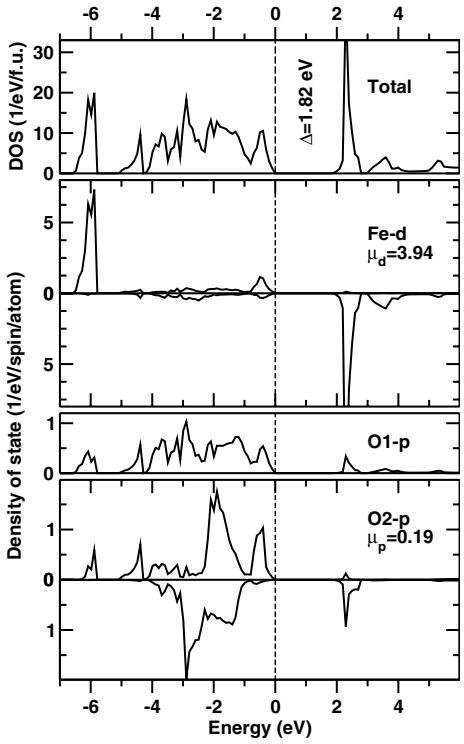

Fig. 3. The total and partial densities of states obtained in LSDA+U calculations with Fe in the high spin state.

effects will not change the quantative results considerably. The criterion of convergence for total energy calculations was 5×10^{-6} eV per supercell.

3 Results and discussion

3.1 Electronic structure and magnetic properties

The LSDA calculations result in a metallic type of the electronic structure for A-type AFM order with the density of states $n(E_F) = 4.3$ states/(eV·formula unit (f.u.)) at the Fermi level. Similar calculations for C-AFM and G-AFM types of magnetic ordering give a semiconductor type electronic structure with the energy gaps of 0.60 eV and 0.64 eV, respectively. The obtained spin magnetic moments of Fe3d ions for different types AFM orders are close to 3.3 μ_B. The analysis of the total energy per formula unit in $Sr_3Fe_2O_6$ with A, C, and G-types of AFM structure shows that the G-type is the most stable. The energy value for G-AFM structure is 0.96 eV/f.u. lower than that for A-AFM order and 1.2 meV/f.u. lower than the total energy for C-type of AFM order in $Sr_3Fe_2O_6$. As an example, the total and partial densities of states in $Sr_3Fe_2O_6$ with G-type of AFM structure are shown in Figure 2. The states near the Fermi level originate mainly from Fe3d states with the admixture of 2p oxygen states. The spin-polarized calculations give an underestimated value for the energy gap (0.64 eV) in comparison with the experimental one (2.3 eV [5]).

The calculations of the electronic structure of $Sr_3Fe_2O_6$ were also carried out by means of the LSDA+U approximation where strong electron-electron correlations were taken into account. This enabled us to obtain the energy gap and other features of the electronic spectrum in more reasonable correspondence with experimental data. As it was mentioned above, the G-type AFM structure is the only satisfying the condition of experimentally determined magnetic superstructure [8]. At the same time, the LSDA total energy value of the C-type AFM order of Fe spins is close to that of the G-type. We have calculated the electronic structure for both C- and G-types of AFM order with Fe ions in high spin configuration within the LSDA+U approximation. The total energy for the G-type is calculated to be 4.7 meV/(f.u.) lower than that for the C-type. Thus, the LSDA+U results duplicate the conclusion about the most stable magnetic ordering of the G-type obtained in frames of the LSDA approach, and further we will describe the results corresponding just for the G-type AFM structure.

We found three stable magnetic solutions for $Sr_3Fe_2O_6$ with the G-type AFM order corresponding to the low spin (LS), intermediate spin (IS) and high spin (HS) states of Fe^{3+} ion. The total and partial densities of states for different spin states of iron are shown in Figures 3–5, the detailed information about calculation results — in Table 2. The semiconductor type electronic structure is obtained for all the solutions. However, variations are observable in the electronic structure of $Sr_3Fe_2O_6$ at changes of the Fe ion spin state.

Table 2. Various spin states of Fe^{3+} ion, calculated occupancies of various d orbitals, magnetic moments, energy gaps and total energy differencies (δ) relative to high spin state configuration in $Sr_3Fe_2O_6$.

Spin		d-occupancies						$\mu_{d-\mathrm{Fe}}$	Energy	δ
state		xy	yz	zx	$3z^2-r^2$	x^2-y^2	total	(μ_B)	gap (eV)	(eV/f.u.)
HS	↑	0.96	0.97	0.97	0.94	0.97	5.68	3.94	1.82	
	↓	0.08	0.13	0.13	0.24	0.29				
IS	↑	0.95	0.96	0.96	0.94	0.39	5.82	2.58	0.91	1.20
	↓	0.93	0.10	0.10	0.26	0.23				
LS	↑	0.94	0.94	0.94	0.31	0.34	5.90	1.04	0.72	1.82
	↓	0.08	0.93	0.93	0.22	0.27				

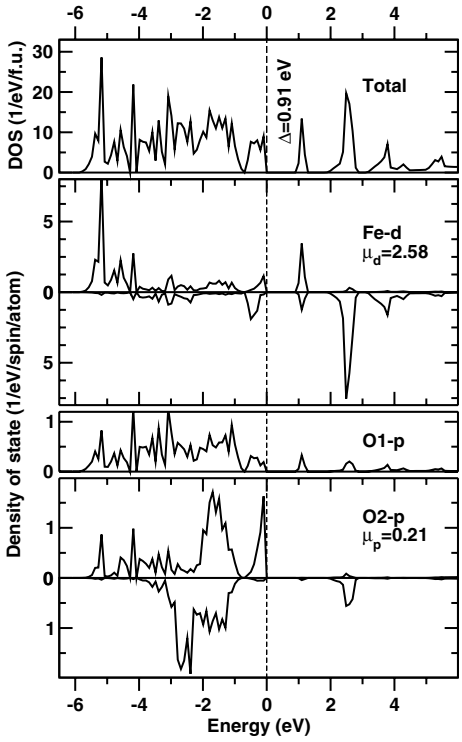

Fig. 4. The total and partial densities of states obtained in LSDA+U calculations with Fe in the intermediate spin state.

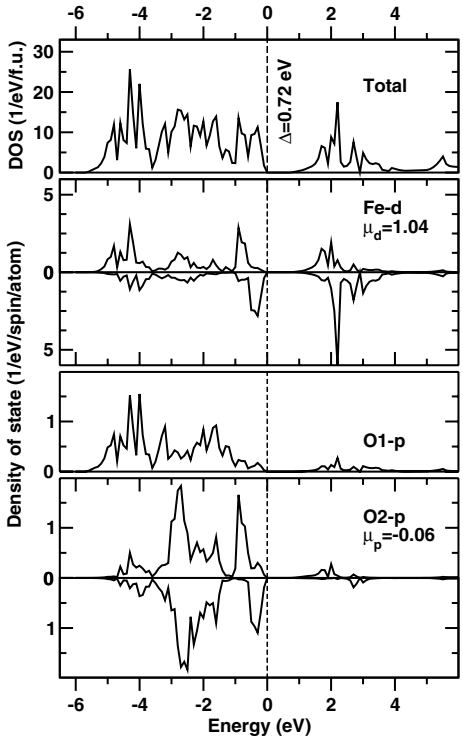

Fig. 5. The total and partial densities of states obtained in LSDA+U calculations with Fe in the low spin state.

The three bands may be seen in electronic spectrum of the HS solution, Figure 3. The low energy band at –6.3 eV consists mainly of Fe3d states. The wide valence band in the interval from –5.3 eV to 0 eV is composed by hybridized O2p-Fe3d states with admixture of 5s, 5p, and 4f states of Sr. The bottom of the conduction band is built mainly of Fe3d states. The lowest Fe3d band that is well separated from other bands in the HS solution now interflows with the valence band in the IS and LS solutions for $Sr_3Fe_2O_6$, Figures 4, 5. The energy gap decreases at transition from the HS to the LS state. The HS solution has the largest value of the energy gap of 1.82 eV. This value agrees reasonably well with the experimental one. It is a charge transfer energy gap (according to the Zaanen-Sawatzky-Allen classification scheme [16]), which separates the occupied valence O2p-like band from the empty conduction Fe3d-like band. The charge transfer type energy gap is also observed for the IS state of iron. At the same time, the energy gap calculated for the LS state of Fe is of Mott-Hubbard type. In this case the energy gap separates the top of the valence band composed essentially by Fe3d states and the empty Fe3d-like conduction band, Figure 5. The total energy of HS state is 1.20 eV/f.u. and 1.82 eV/f.u. smaller than that of the IS and LS states, respectively. Thus, the HS state is energetically most favorable for $Sr_3Fe_2O_6$.

The analysis of the occupation matrix of iron obtained in the LSDA+U calculations for HS state (Tab. 2) results in the following features i) the value of the local spin magnetic moment of iron is equal to 3.94 μ_B; ii) the Fe3d states have $t_{2g}^{3\uparrow}e_g^{2\uparrow}e_g^{1\downarrow}$ configuration; iii) the occupation of Fe3d shell is 5.7 e, which is not typical for trivalent ion of iron. In the ionic model the HS state of Fe^{3+} ion is described as $t_{2g}^{3\uparrow}e_g^{2\uparrow}$ configuration with the spin value of

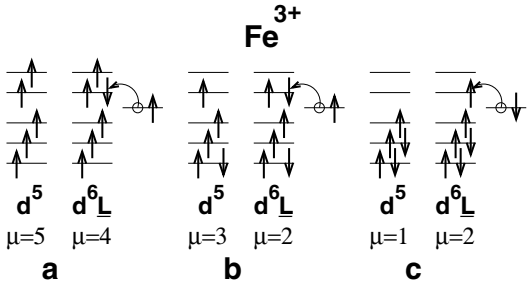

Fig. 6. The schematic representation of Fe $d^5 + d^6L$ configurations in the high (a), intermediate (b) and low (c) spin states. The open circle denotes a hole in the oxygen $2p$ state.

$S = 5/2$ (spin magnetic moment $\mu_{Fe} = 5\ \mu_B$), left side of Figure 6a. However, the strong hybridization of Fe3d orbitals with oxygen $2p$ orbitals, which is typical for strontium ferrites [11], can renormalize significantly this ionic value of the spin. In this case the electron with opposite spin could pass from oxygen p orbital to the empty e_g orbital of Fe, right side of Figure 6a. The O(2) p orbitals form σ bonds with e_g type orbitals and π bonds with t_{2g} orbitals of iron in FeO_5 square pyramids, thus making easier the transition of electrons from O(2) p orbital to Fe e_g orbital. Such argumentation is fully supported by numerical data of orbital occupancies calculated for HS solution (Tab. 2). This transfer allows one to explain the existence the HS trivalent iron with the spin magnetic moment close to 4 μ_B. In a configuration-interaction language used in the cluster calculations, the HS state can be described as $d^5 + d^6L$, where L denotes a hole on the oxygen, with domination of d^6L states.

The removal of the O(3) oxygen atoms linking iron-oxygen octahedra along c axis strongly influences the exchange magnetic interactions between iron ions in $Sr_3Fe_2O_6$. Following prescription of work [17], we computed the Heisenberg model exchange interaction parameters between nearest Fe ions in ab plane and nearest Fe ions belonging to the different planes in c direction. For the HS solution, the in-plane constant J_{ab} is equal to 109.5 meV, while the inter-plane constant J_c achieves only 9.5 meV; both of them correspond to antiferromagnetic interaction.

The Fe ion in the IS state in our calculations, Figure 4, has the spin magnetic moment value $\mu_{Fe} = 2.58\ \mu_B$, and the occupancy of Fe3d shell is equal to 5.8 e. This result can be compared with $d^5 + d^6L$ configuration with practically equal contributions from both states, Figure 6b.

The spin magnetic moment for the LS state, Figure 5, is 1.04 μ_B, which corresponds to d^5 configuration with a very small admixture of d^6L states, Figure 6c. The contribution from d^6L configuration is confirmed by a small negative spin moment on O2p shell, which is calculated to be opposite to the moments on Fe3d shell.

During the calculations we tried to find both the charge or orbital order of Fe ions and the coexistence of Fe ions in the different spin states. Our attempts were unsuccessful. Only three stable solutions for strontium ferrite $Sr_3Fe_2O_6$ were found in frames of the LSDA+U approach as described above.

Table 3. The total energy difference (relative to the energy of the configuration b in Fig. 7) for different mutual positions of two oxygen vacancies in $Sr_3Fe_2O_6$. d is the distance between the vacancies. The supercell under consideration consisted of 2 formula units.

Configuration	Part of Figure 7	d, Å	ΔE, eV/supercell
$V_{O(3)}$–$V_{O(1)}$	b	2.578	0.00
$V_{O(3)}$–$V_{O(2)}$	c	3.934	2.04
$V_{O(1)}$–$V_{O(1)}$	d	3.378	0.14
$V_{O(1)}$–$V_{O(1)}$	e	4.358	0.36
$V_{O(1)}$–$V_{O(1)}$	f	5.155	0.60
$V_{O(1)}$–$V_{O(2)}$	g	5.951	3.96
$V_{O(1)}$–$V_{O(1)}$	h	2.753	1.80
$V_{O(1)}$–$V_{O(1)}$	i	3.893	0.84
$V_{O(1)}$–$V_{O(2)}$	j	2.971	4.28

3.2 Transport properties

The $Sr_3Fe_2O_6$ compound is mixed oxygen-ion and electron conductor with the oxygen-ion conductivity level achieving 0.06 S/cm at high temperatures. It is suggested in work [5] that the mechanism underlying oxygen ion transport is related to the temperature driven position exchange of oxygen vacancies in O(3) sites and oxygen anions in either O(1) or O(2) sites. The mechanism of the oxygen transport in $Sr_3Fe_2O_6$ can be presented in analogy to that in $Sr_3Fe_2O_5$ [18]. According to this mechanism, the O(1), O(2) oxygen atoms in $Sr_3Fe_2O_6$ can be transferred at heating to the empty O(3) sites. This corresponds to the formation of anti-Frenkel pairs (AFP) in the reactions:

$$V_{O(3)} + O(1) = O(3)_i + V_{O(1)} \quad (1)$$

$$V_{O(3)} + O(2) = O(3)_i + V_{O(2)} \quad (2)$$

where $O(3)_i$, $V_{O(1)}$, $V_{O(2)}$, and $V_{O(3)}$ are the interstitial oxygen and oxygen vacancies, respectively. Then the transfer of the generated oxygen vacancies to O(1), O(2) sites is possible. In order to probe the viability of this disordering, we carried out the LSDA+U calculations for several possible configurations, Figure 7, of two oxygen vacancies in G-AFM ordered $Sr_3Fe_2O_6$.

Figure 7 illustrates the fragments of the ideal a and defect structures with the AFP: interstitial oxygen $O(3)_i$ and oxygen vacancy $V_{O(1)}$ for the configuration b or $V_{O(2)}$ for the configuration c. Configurations b and c correspond to the presented above the anti-Frenkel disordering reactions (1) and (2), respectively. The AFP formation energies for the reactions are calculated to be 2.8 eV and 4.8 eV. Therefore, the anti-Frenkel disordering via reaction (1) is energetically most favorable.

The distribution of the generated oxygen $V_{O(1)}$ vacancies over O(1) and O(2) sites was also investigated. The total energy differences (relative to the energy of the configuration b) for all kinds of configurations are given in Table 3.

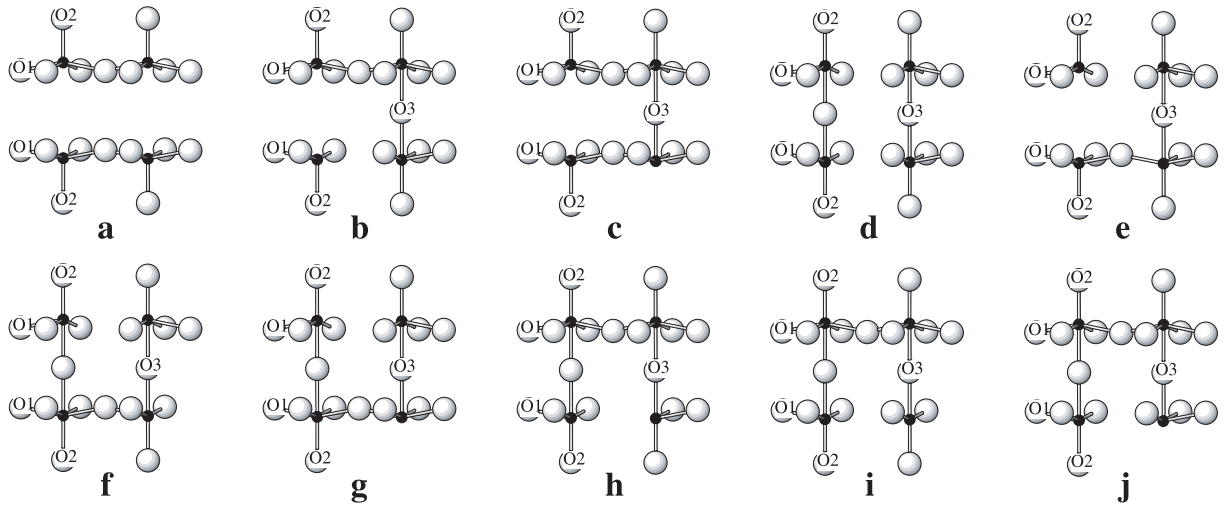

Fig. 7. The fragment of the double layers of FeO_5 pyramids with two oxygen vacancies on O(3), on O(1) or on O(2) sites for ideal (a) and defect configurations (b)–(j). Iron atoms are depicted as black dots surrounded by grey balls of oxygen ions. Strontium atoms are not shown.

Four configurations (from d to g) correspond to the mutual position of two oxygen vacancies in the near-neigh-bour layers in the perovskite block. Configurations d–f have two oxygen vacancies on O(1) sites. The $V_{O(1)}$–$V_{O(1)}$ distance is increased at transition from the configuration d to the configuration f. Configuration g consists of one oxygen vacancy on O(1) site and another one on O(2) site at the distance of 5.951 Å. The calculation results for these configurations (Tab. 3) show that: i) the total energy difference, ΔE, for the configurations d–f increases with the $V_{O(1)}$–$V_{O(1)}$ distance, i.e. the configuration d is energetically more favorable; ii) the ΔE for the configuration d–f does not exceed 0.46 eV per supercell; iii) the configurations d–f with the oxygen vacancies distributed over O(1) sites are more preferable than the configuration g with $V_{O(2)}$ vacancy. Thus, the transfer of the oxygen vacancies via O(1) sites is energetically most favorable.

The three hypothetical configurations h–j of oxygen vacancies in the same layer of $Sr_3Fe_2O_6$ block were calculated. Configurations h and i contain two oxygen vacancies of the same type $V_{O(1)}$ and differ from each other by the $V_{O(1)}$–$V_{O(1)}$ distance. The distance increases from 2.75 Å for the configuration h to 3.89 Å for the configuration i (Tab. 3). The configuration j has two oxygen vacancies $V_{O(1)}$ and $V_{O(2)}$ of different types. It is seen from Table 3 that the total energy difference for the configurations h and i is more than two times smaller than that for the configuration j, i.e. the first two configurations are more energetically favorable. The energy difference between the configurations h and i achieves of about 1 eV (Tab. 3). This fact gives evidence to the attraction between the oxygen vacancies at a short distance.

Thus, the calculation results show that the configurations with oxygen vacancies disordered over O(3) or O(1) sites are most energetically favorable (the configurations b, d–f). The analysis of calculations allows to suggest that i) the oxygen transport is most preferable through the vacant $V_{O(1)}$ sites after formation of anti-Frenkel pairs and ii) the ion transport in the strontium ferrite is triggered by the position exchange of oxygen ions and oxygen vacancies through O(1) sites. However, the AFP formation energies obtained in our calculations could be considered as probably uppur bounds, since any lattice relaxation was out of our current consideration.

4 Conclusions

The electronic structure and magnetic properties of strontium ferrite $Sr_3Fe_2O_6$ were calculated with the use of TB LMTO ASA band structure method in the LSDA+U approximation. The calculations show that the HS state of trivalent Fe ion with unusual spin magnetic moment of 3.94 μ_B is the most stable. The strong hybridization of Fe3d-O2p orbitals results in suppression of the magnetic moments of Fe ions to $\sim$4 μ_B. The HS state of trivalent iron can be described as a mixture of d^5 and d^6L configurations with prevalence of the last one. The calculated charge transfer gap in $Sr_3Fe_2O_6$ is 1.82 eV. The in-plane Fe-Fe exchange magnetic interaction is one order of magnitude larger than that between the nearest inter-plane in the double perovskite block. The calculation results also show that the important prerequisite for oxygen ion transport in $Sr_3Fe_2O_6$ involves position exchange of oxygen ions and oxygen vacancies through the nearest O(1) sites.

We would like to thank Dr. I.A. Leonidov for valuable discussions. The research is supported by the Russian Science Support Foundation, the RF Ministry of Education and Science and the CRDF Annex BF4M05, EK−005−X2 [REC−005], BRHE 2004 post-doctoral fellowship Y2−E−05 − 17 and the RFBR 04-02-16096, 04-03-32948a grants.

References

1. S. Ghosh, P. Adler, J. Mater. Chem. **12**, 511 (2002)
2. M.A. Patrakeev, I.A. Leonidov, V.L. Kozhevnikov, V.V. Kharton, Solid State Sci. **6**, 907 (2004)
3. F. Prado, A. Manthiram, J. Solid State Chem. **158**, 307 (2001)
4. P. Adler, J. Mater. Chem. **9**, 471 (1999)
5. Y.A. Shilova, M.V. Patrakeev, E.B. Mitberg, I.A. Leonidov, V.L. Kozhevnikov, K.R. Poeppelmeier, J. Solid State Chem. **168**, 275 (2002)
6. K. Kuzushita, S. Morimoto, S. Nasu, S. Nakamura, J. Phys. Soc. Jpn **69**, 2767 (2000)
7. K. Kuzushita, S. Morimoto, S. Nasu, Phys. B **329**–**333**, 736 (2003)
8. K. Mori, T. Kamiyama, H. Kobayashi, T. Arima, K. Ohoyama, S. Ikeda, Appl. Phys. A. **74**, S914 (2002)
9. T. Kobayashi, M. Kira, H. Onodera, T. Suzuki, T. Kamimara, Phys. B **237**–**238**, 105 (1997)
10. S.E. Dann, M.T. Weller, D.B. Currie, M.F. Thomas, A.D. Al-Rawwas, J. Mater. Chem. **3**, 1231 (1993)
11. M. Abbate, H. Ascolani, F. Prado, A. Caneiro, Solid State Commun. **129**, 113 (2004)
12. S.E. Dann, M.T. Weller, D.B. Currie, J. Solid State Chem. **97**, 179 (1992)
13. V.I. Anisimov, F. Aryasetiawan, A.I. Lichtenstein, J. Phys.: Condens. Matter **9**, 767 (1997)
14. O.K. Andersen, Z. Pawlowska, O. Jepsen, Phys. Rev. B **34**, 5253 (1986)
15. I. Leonov, A.N. Yaresko, V.N. Antonov, M.A. Korotin, V.I. Anisimov, Phys. Rev. Lett. **93**, 146404 (2004)
16. J. Zaanen, G.A. Sawatzky, J.W. Allen, Phys. Rev. Lett. **55**, 418 (1985)
17. A.I. Lichtenstein, V.I. Anisimov, J. Zaanen, Phys. Rev. B **52**, R5467 (1995)
18. V.M. Zainullina, I.A. Leonidov, V.L. Kozhevnikov, Phys. Solid State **44**, 2063 (2002) (translated from Fizika Tverdogo Tela **44**, 1970 (2002))